Journal of Radiotherapy in Practice

cambridge.org/jrp

Dosimetric effect of modelling non-homogeneous LINAC couch using cone-beam computed tomography on quality assurance (QA) results

Amin Banaei[1], Mohsen Bakhshandeh[2] and Mohammad Rasa Golrokh-Nodehi[3]

[1]Department of Medical physics, Faculty of Medical Sciences, Tarbiat Modares University, Tehran, Iran; [2]Department of Radiology Technology, Faculty of Allied Medical Sciences, Shahid Beheshti University of Medical Sciences, Tehran, Iran. and [3]Department of Medical Radiation Engineering, Science and Research Branch, Islamic Azad University, Tehran, Iran

Original Article

Cite this article: Banaei A, Bakhshandeh M, and Golrokh-Nodehi MR. (2023) Dosimetric effect of modelling non-homogeneous LINAC couch using cone-beam computed tomography on quality assurance (QA) results. *Journal of Radiotherapy in Practice*. **22**(e31), 1–13. doi: 10.1017/S1460396921000716

Received: 23 June 2021
Revised: 12 November 2021
Accepted: 30 December 2021

Key words:
intensity-modulated; quality assurance; radiotherapy; volumetric modulated arc therapy; treatment couch

Author for correspondence:
Mohsen Bakhshandeh, Department of Radiology Technology, Faculty of Allied Medical Sciences, Shahid Beheshti University of Medical Sciences, Tehran, Iran.
Email: Mbakshandeh@sbmu.ac.ir

Abstract

Aim: To evaluate the dosimetric effect of modelling a non-homogeneous couch on patients' quality assurance (QA) gamma pass rates for intensity-modulated radiotherapy (IMRT) and volumetric modulated arc therapy (VMAT) techniques.

Materials and Methods: A non-homogeneous treatment couch (TxT 550 TTM, CIVCO, USA) was imaged using the LINAC mounted cone-beam computer tomography (CBCT) system. Modelling this couch in different situations, including incomplete (homogeneous model), correct model and not defined situations in the treatment planning system (TPS), was performed based on the geometrical and material densities data extracted from the CBCT images. Calculated gamma pass rates between TPS dose calculations and the measurements in a phantom for different couch models were obtained and compared at two gamma criteria (2%-2 mm and 3%-3 mm).

Results: Comparing TPS calculations for the correct modelled couch and the measurements showed high gamma pass rates for both the IMRT and VMAT techniques (96·5 ± 0·9%, 99·2 ± 0·5% for IMRT in 2%-2 mm and 3%-3 mm criteria; 97·5 ± 0·8%, 99·4 ± 0·5% for VMAT). The overall gamma pass rate of the IMRT plan QAs was reduced by about 2% and 3% on average for incomplete and no couch modelling, respectively. These reductions for VMAT techniques were 2·5% and 4·3%, respectively.

Conclusions: Non-homogeneous couches have different parts with different attenuations, which can be correctly defined using LINAC CBCT. Modelling of treatment couch has a significant effect on patient QA results for VMAT and IMRT plans, especially in radiation fields/subfield transmitting from the couch. We suggest using LINAC CBCTs as an appropriate device for couch modelling in modulated radiotherapy techniques.

Background

Modulated radiotherapy techniques such as intensity-modulated radiotherapy (IMRT) and volumetric modulated arc therapy (VMAT) are now commonly used in radiotherapy. The use of intensity-modulated radiations resulted in highly conformal dose distribution to the target and reduced dose to adjacent organs at risk.[1] In this technique, planning target volume margins can usually be reduced, and doses to organs at risk can be decreased due to the sharp drop off from the target.[2,3] Because of higher conformity and dose gradient in modulated radiotherapy techniques compared to conventional and 3D conformal techniques, patients' radiation dose distribution can be more impacted by the treatment couch top and supporting devices. Therefore, more accurate patient radiation dose distribution could be achieved if the treatment couch is incorporated in the treatment planning system (TPS) dose calculations. This can be accomplished by modelling the couch and the supporting devices in the TPS.

Couch materials are now mainly constructed from carbon fibre; however, there are some treatment couches constructed from different materials such as carbon fibre, copolyester and aluminium alloy (e.g., 550 TxT TTM CIVCO couch, USA). Carbon fibre is more radio-translucent[4] and provides lower attenuation for high energy photon beams compared to hardboard, copolyester and polymethylmethacrylate.[5–7] Inhomogeneous treatment couches may be composed of different materials (carbon fibre, glass fibres or metal(and regions with different thicknesses having high attenuations in some parts, especially in the parts that are irradiated with posterior oblique fields.[8,9] Thicker or denser regions are located at the edges of the couch, and posterior oblique beams go through these regions.

For homogeneous treatment couches with uniform thickness, a single attenuation factor is usually implemented for posterior fields. However, it is more accurate to use CT images of the couch for couch modelling in the TPS. Vendors provide CT images of couch/couch tops for some commercial models; in contrast, most coaches have no CT images. Therefore, these couches must be modelled in TPS, and the necessary data, including geometry and densities, can be obtained using CT [(or cone-beam computer tomography (CBCT)] imaging. Separating couch parts from the couch system is relatively hard and time-consuming and may result in further misalignment. Using of CBCT system of the LINAC may be an appropriate approach to obtain couch CT images without disassembling the couch.

According to the recommendations of American Association of Physics in Medicine (AAPM) task group 142 report,[10] pre-treatment patient quality assurance (QA) must be performed for modulated radiotherapy techniques to ensure that the planned dose distribution is similar to the dose distribution that will be delivered to the patient. The measured dose distributions (as a reference) usually are compared with TPS calculations (calculated dose) using the gamma analysis. The gamma pass rate obtained from the gamma analysis is a good predictor for evaluating the similarity of delivered dose with the TPS calculated dose distribution.[10] In this study, we used the gamma analysis concept to evaluate the effect of treatment couch modelling on the planned dose distribution by comparing both the predicted (TPS calculated) and measured doses for IMRT and VMAT techniques. Furthermore, we used a relatively simple method for treatment couch modelling using LINAC mounted CBCT and presented the validation procedure in this study.

Methods

A single-centre, retrospective study was done after national research ethics board approval.

Couch imaging

The 500 TxT TTM couch (CIVCO, USA) is a multipurpose couch with different interchangeable couch panels, including solid, grid and tangential grid panels. This couch with a grid panel was imaged using Artiste linear accelerator CBCT (ARISTE Precision, Siemens, Germany) through a 360° arc [field of view (FOV): 27 × 27 cm^2)]. The couch's lateral dimension (53 cm) was bigger than the imaging maximum lateral FOV; therefore, the right and left regions of the couch were scanned separately. Averaged Hounsfield units (HUs) from different parts were obtained by defining the appropriate regions of interest (ROIs) on the couch's CT images using ImageJ software (National Institutes of Health, USA). These values were used to find the average mass density for different parts using the CT calibration curve of the CBCT. Mass density values were imported to the RayStation TPS (RaySearch company, Sweden) to calculate the attenuation of the couch.

HU calibration of LINAC mounted CBCT

The RT-smartCTQA (dose.point GmbH, Germany) phantom was used to find the relationship between the HU obtained from the CBCT and mass/electron density of different materials. This phantom consists of different cylindrical rods with known materials (Air, RW3, Acrylic, titanium, lung equivalent material, muscle and adipose equivalent materials) positioned in a 300 × 300 × 70 mm^2 RW3 cube.

CBCT imaging of this phantom was carried out using a 1 MV X-ray beam with a 358° arc (181–179 clockwise) and OPTIVUE 1000ART a-Si flat panel system as an image detector. The FOV was 27 × 27 cm^2 reconstructed slice thickness of 0·7 cm.

HUs of different materials were measured using averaging Hounsfield values in circular ROIs in a transversal slice of the phantom for each material. ImageJ software (National Institutes of Health, USA) was used to calculate the average HU values.

HU values obtained from kilovoltage CT scans are commonly used to determine the mass or electron density values used for dose calculations in TPS. However, the HU values obtained from the MV-CBCT are accurate enough for dose calculations due to the calibration process and finding a relationship between HU and mass density.[11–13]

Modelling of treatment couch in the TPS

CBCT images of the couch were imported to the TPS (Ray Station, V.8.a, RaySearch Company, Sweden). Different parts of the table were contoured manually. A 3D reconstructed image of the couch, as shown in Figure 1, shows different parts of the modelled couch.

In our study, three different parts were contoured separately for the couch, including the middle part of the panel, outer part of the panel (panel edges) and couch frame. The mass densities obtained from the CBCT relative electron density curve were manually assigned to the different parts of the couch. The middle part and frame of the couch were composed of different materials, but we used a mean mass density for each part of the model for simplicity.

Three different couch models were assessed to evaluate the effect of correct treatment couch modelling on the patient QA results. In the first situation, just the couch panel was imported and considered that all the parts were homogeneous (homogeneous or incomplete model). In another situation, all couch parts, including the couch frame and couch panel consisting of middle thinner part, and peripheral thicker regions (with higher mass density), were considered and imported (in-homogeneous or correct model). In the third model, no couch was considered to estimate couch effect on patients' QA gamma pass rates.

To evaluate the treatment couch modelling, several radiation fields (5 × 5 cm^2, 10 × 10 cm^2 and 20 × 20 cm^2) with two photon energies (6 MV and 7 MV flattening filter-free) at different gantry angles irradiating to asymmetrical cylinder phantom (OCTAVIUS 4D phantom with standard top of this phantom) were simulated in the TPS. Results of measurements were compared with the TPS calculations. The OCTAVIUS phantom with a 30 × 30 × 2 cm^3 RW3 slab was positioned in the centre of the phantom. A PTW farmer type chamber (sensitive volume = 0·6 cm^3, PTW company, Germany) was positioned inside the slab in the centre of the phantom. This phantom is composed of a stationary base, and a cylindrical volume rotated synchronously with gantry based on the angular data measured by an inclinometer. This causes the phantoms' top to be always perpendicular to the radiation field, making more accurate dosimetry with similar phantom conditions in different gantry angles.

Treatment planning and patient QA procedure

Twenty-two treatment plans, including 12 VMAT (with 2–4 arcs for each plan) and 10 IMRT (with 6–9 fields for each plan) plans, were used to evaluate the effect of couch modelling on the QA results.

https://doi.org/10.1017/S1460396921000716 Published online by Cambridge University Press

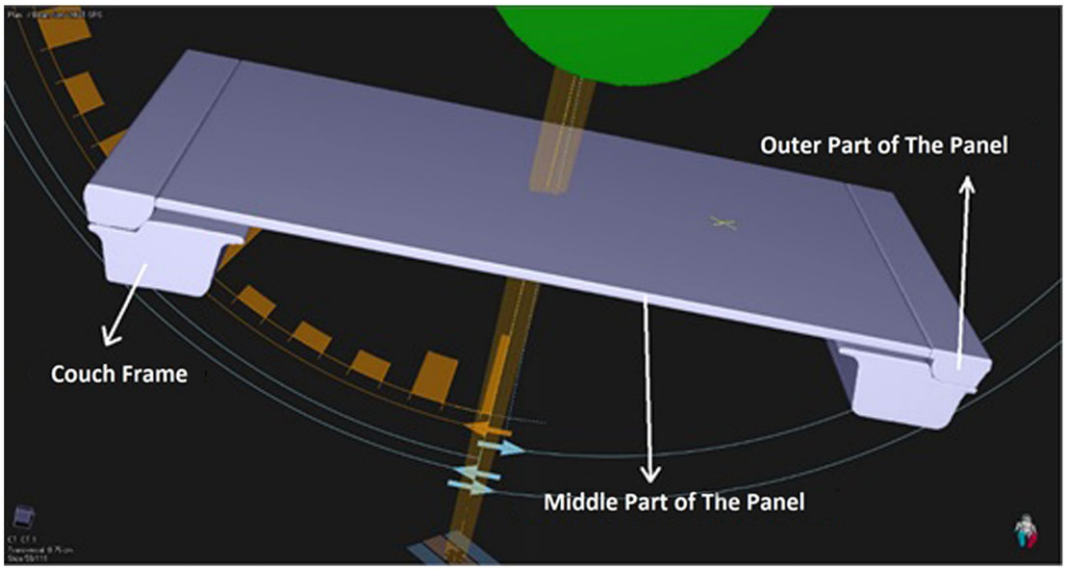

Figure 1. A 3D reconstructed image of the modelled couch showing different parts.

All of the treatment plannings were performed using RayStation TPS (V.8.a, Sweden), which was previously commissioned for IMRT techniques according to the TG-119 report of AAPM.[14] Furthermore, quality control and commissioning of VMAT procedures were performed based on the Report 24 of the Netherlands Commission on Radiation Dosimetry.[15]

All the patient IMRT/VMAT and stereotactic radiotherapy QA plans were measured using the OCTAVIUS 4D (PTW company, Germany) modular phantom with the PTW 2-D array detector 1500 and detector 1000 SRS (PTW company, Germany), respectively. We used the standard head top (diameter = 32 cm) for IMRT and VMAT techniques, and the SRS head top, which has a smaller diameter of 17 cm, was used for stereotactic VMAT plans. The vendor-supplied CT images of the phantom (with different tops) were imported to the TPS. Couch models were also imported and positioned under the phantom with known physically measured distances between the phantom and treatment couch.

The OCTAVIUS 4D phantom was scanned and exported to the TPS to calculate dose distribution. The collapsed cone photon dose calculation engine was used by the TPS as the dose calculation algorithm for all of the patients' treatment plans and also dose calculations in the OCTAVIUS 4D phantom for QA purposes. Dose grids of $2 \times 2 \times 2$ mm^3 and $1 \times 1 \times 1$ mm^3 were used for calculations in OCTAVIUS 4D phantom with standard and SRS head top, respectively. Lower dose grid dimensions were used for smaller phantom and field sizes for higher accuracy.

The TPS calculated plans were irradiated to OCTAVIUS 4D phantom, and the irradiation fluences in different gantry angles were measured with this phantom. After measurements, the dose distributions in three dimensions inside the phantom were calculated based on the fluence measurements at different gantry angles. All the measurements were done at zero couch angle to avoid exposing the electronic parts of the detector to direct radiation.

Gamma analysis

After measuring the irradiated fluences for each field/arc, the 3D dose distribution for each field/arc and all the fields/arc for each plan were obtained in the phantom volume using VeriSoft software (Version 7.0, PTW Company, Germany). A convolution-based algorithm (developed by PTW company) was used to obtain volumetric dose distribution from measurements obtained at different gantry angles by the method described in Allgaier et al. study.[16] Then, the 3D gamma analysis between the TPS calculated and measured dose distributions in OCTAVIUS 4D phantom was performed for each field using two criteria, including the 2%/2 mm and 3%/3 mm dose difference/distance to the agreement. The global maximum dose was used as the normalisation value for both the measured and planned dose distributions. The gamma values were calculated in the regions with doses higher than the threshold value (10% of the maximum dose). The gamma pass rates obtained from the QA procedures with different couch models were compared using the repeated measurement statistical test. The significant level was considered as p-value $< 0{\cdot}05$. All statistical analyses were performed using the SPSS software (Version 12, IBM, USA).

Results

Calibration of CBCT

The averaged mass densities of the middle part of the couch top, outer part of the couch top and couch frame were $0{\cdot}03 \pm 0{\cdot}01$, $0{\cdot}9 \pm 0{\cdot}15$ and $0{\cdot}1 \pm 0{\cdot}01$, respectively. The calibration curve was used to estimate the mass densities of different parts of the treatment couch, and these average mass densities were assigned manually to the couch.

Validation of treatment couch

We measured the attenuation of the couch in different gantry angles to show its high attenuation values in some angles. The radiation fields transmitted through the edge of the couch (gantry angles: 130–150° and 210–230°) have about 10–12% more attenuation than the anterior field (gantry angle = 0). Couch attenuations in the posterior field (gantry = 180) were between 2·1 and 3·4% for different field sizes and energies. Therefore, if the couch will be defined homogeneously based on the middle part's attenuation, posterior oblique fields will have about 7% dose

https://doi.org/10.1017/S1460396921000716 Published online by Cambridge University Press

Table 1. The results of chamber readout differences between obtained values in different gantry angles with values obtained in zero gantry angle at different field sizes for two investigated photon energies (6 MV and 7 MV FFF). All values were presented in percentage

	6 MV			7 MV FFF		
Gantry angle	5 × 5 cm^2	10 × 10 cm^2	20 × 20 cm^2	5 × 5 cm^2	10 × 10 cm^2	20 × 20 cm^2
0	0	0	0	0	0	0
45	0	0	0	0	0	0
90	0	0	0	0	0	0
100	1·8	1·6	1·6	1·5	1·6	1·5
110	3·8	3·5	3·3	2·4	2·4	2·3
120	10·1	9·2	8·6	8·4	8·1	7·7
130	12·1	11·8	11·2	10·8	10·6	10·1
140	12·5	12	11·6	11·1	10·9	10·4
150	11·6	10·9	10·3	9·9	9·7	9·3
160	7·7	7·3	6·9	6·4	6·2	5·9
170	4·4	4·1	3·8	2·7	2·6	2·4
180	3·4	3·2	3·1	2·3	2·2	2·1
190	5·8	5·4	5·1	4·6	4·4	4·2
200	7·7	7·2	6·8	6·1	5·9	5·6
210	10·3	9·7	9·2	8·8	8·5	8·1
220	12·4	12	11·5	11	10·6	10·1
230	12·4	11·9	11·2	10·7	10·3	9·8
240	10·9	10·3	9·8	9	8·7	8·3
250	3·7	3·5	3·3	2·7	2·6	2·4
260	2	1·8	1·7	1·5	1·5	1·4
270	0	0	0	0	0	0
315	0	0	0	0	0	0

calculations error at isocentre in TPS. Table 1 shows the results of chamber readout differences between obtained values in different gantry angles with values obtained in zero gantry angle at different field sizes for two investigated photon energies.

Gamma pass rate results for IMRT and VMAT patients QA

Figures 2 and 3 show the overall gamma pass rate results of IMRT and VMAT patients' QAs, respectively, for three couch models conditions at two gamma criteria (2%-2 mm and 3%-3 mm).

The average ± standard deviation (SD) gamma pass rate percentage for IMRT patients pre-treatment plan QAs in 2% and 2 mm gamma criteria were 96·49 ± 0·88, 94·55 ± 1·77 and 93·53 ± 2·75 for correct, incomplete and no couch definitions, respectively. These values for 3% and 3 mm limitations were 99·16 ± 0·52, 97·59 ± 1·68 and 97·13 ± 2·06.

The average±SD values of gamma pass rate percentage for VMAT patients pre-treatment QA plans in 2% and 2 mm gamma analysis criteria were equal to 97·54 ± 0·83, 95·02 ± 0·87 and 93·15 ± 1·29 for incomplete, correct and no couch models, respectively. These values for 3% and 3 mm criteria were 99·45 ± 0·46, 96·62 ± 0·64 and 94·93 ± 1·39. These values are presented in Figure 8, and the significant statistical differences between the values are marked with the '*' sign. In IMRT (Figure 4a) and VMAT (Figure 4b) techniques in both gamma criteria, in-correct couch modelling in TPS resulted in significantly higher gamma pass rates compared to incomplete and no couch models. Furthermore, the gamma pass rate resulted from comparing measurements with the TPS calculations with incomplete and no couch models did not show significant differences with each other in IMRT QA plans.

Field by field (arc by arc) and plan (all fields together) gamma analysis results for each patient are given in the Appendix section for different gamma analysis criteria and both of the VMAT and IMRT techniques.

The weights of radiation beams (monitor units of each field divided into the monitor units of all fields) for each field were calculated in the TPS. The effect of radiation beams weights transmitting through the treatment couch on the gamma pass rate for IMRT QA plans was also evaluated to evaluate the impact of the IMRT posterior fields contribution to the overall gamma analysis results. Differences of gamma pass rate values between the incomplete couch model with correct and no couch models versus these weight values are shown in Figure 5. For the plans having higher weights, the differences were increased. These differences followed a linear model in 2%-2 mm gamma criteria very well but not a good linear model in 3%-3 mm gamma criteria.

Discussion

In non-homogenous treatment couches, it is not practical to apply one attenuation coefficient for all the couch parts. Therefore,

https://doi.org/10.1017/S1460396921000716 Published online by Cambridge University Press

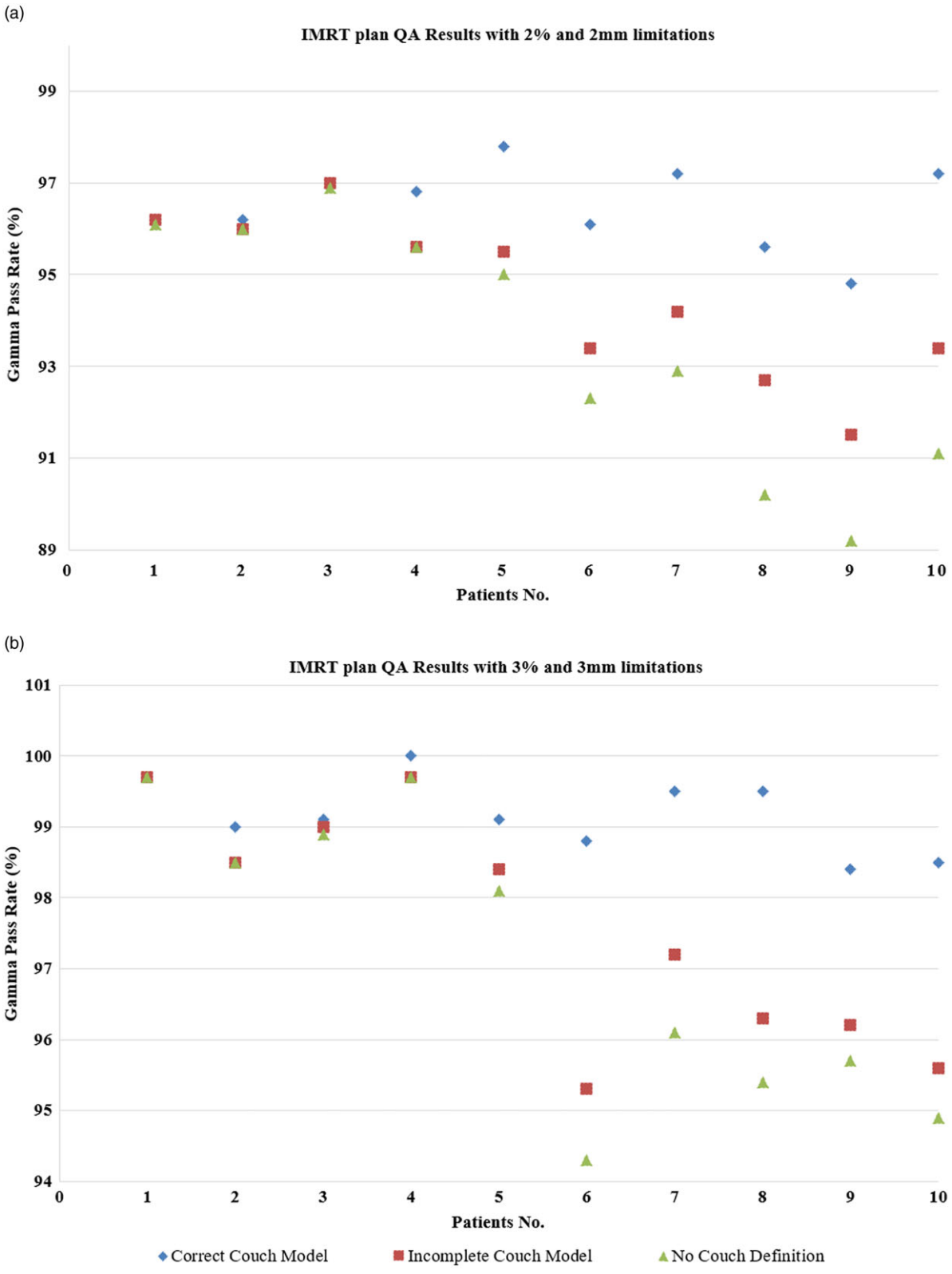

Figure 2. The gamma pass rate results of IMRT QA plans (sum of all fields in each plan) with different situations of couch definition for all the patients at 2%-2 mm gamma criteria (a) and 3%-3 mm gamma criteria (b).

we modelled the treatment couch using LINAC mounted CBCT. For homogeneous couches, the transmission lengths of radiation beam through the couch for posterior oblique fields are significantly longer than the length for posterior fields (gantry = 180). Therefore, it will be more appropriate to model the couch using its CT images instead of considering a single attenuation factor. It was shown that homogeneous couch modelling (incomplete model) resulted in a significant decrease in the QA gamma pass

https://doi.org/10.1017/S1460396921000716 Published online by Cambridge University Press

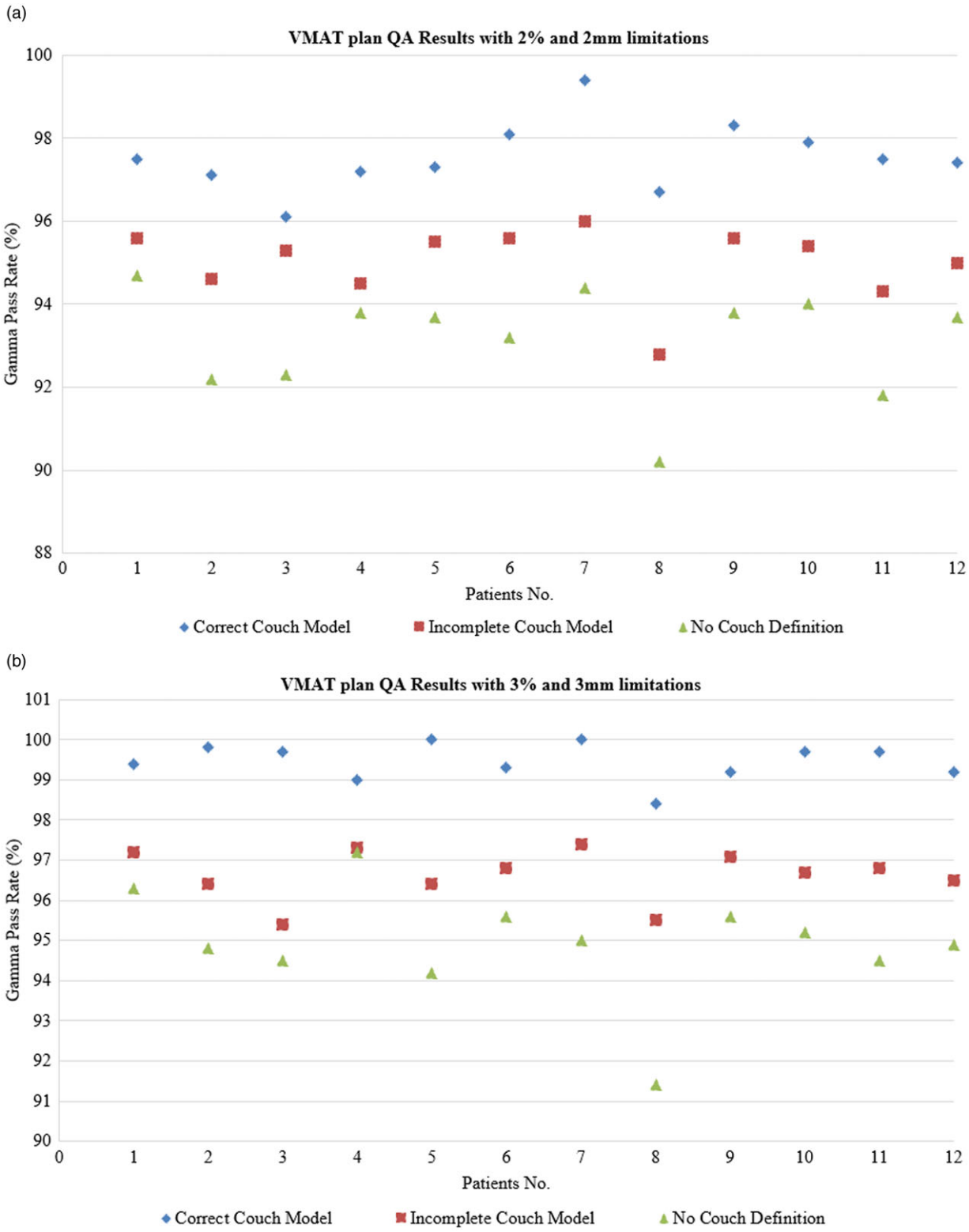

Figure 3. The gamma pass rate results of VMAT QA plans (sum of all arcs in each plan) with different situations of couch definition for all the patients at 2%-2 mm gamma criteria (a) and 3%-3 mm gamma criteria (b).

rates for IMRT and VMAT. Furthermore, treatment couch modelling had higher effects on the QA results of IMRT plans to have higher weights for radiations delivered from posterior directions.

There are several reports evaluating the validation of treatment couches modelling in TPS.[8,9,17–19] In a study by Njeh et al.,[8] the BrainLAB couch top has been modelled in Philips Pinnacle and BrainLAB iPlan RT Dose TPSs. They demonstrated an excellent agreement (1% for all gantry angles measured except for 120°, which was 1·8%) between the measured dose and Pinnacle TPS computed dose using 6 MV photon beams. Predicted attenuation

https://doi.org/10.1017/S1460396921000716 Published online by Cambridge University Press

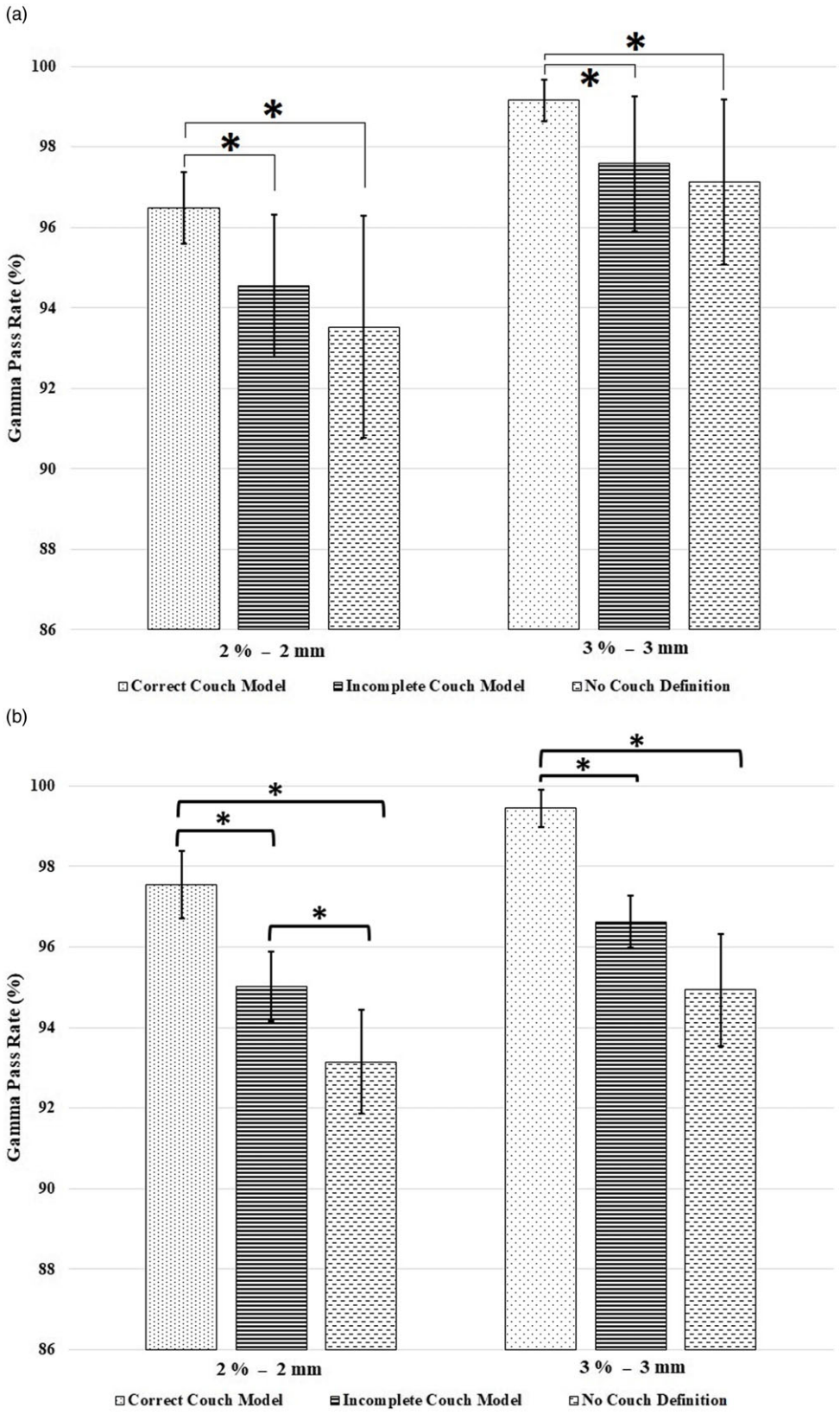

Figure 4. Average gamma pass rate percentage for comparing TPS calculated dose distribution with measurements for IMRT (a) and VMAT (b) pre-treatment QA plans in 2%-2 mm and 3%-3 mm gamma criteria at different situations of couch modelling in the TPS, including incomplete model, correct model and no couch definition. Error bars illustrate standard deviation values.
*: significant differences between groups (p-value < 0·05).

https://doi.org/10.1017/S1460396921000716 Published online by Cambridge University Press

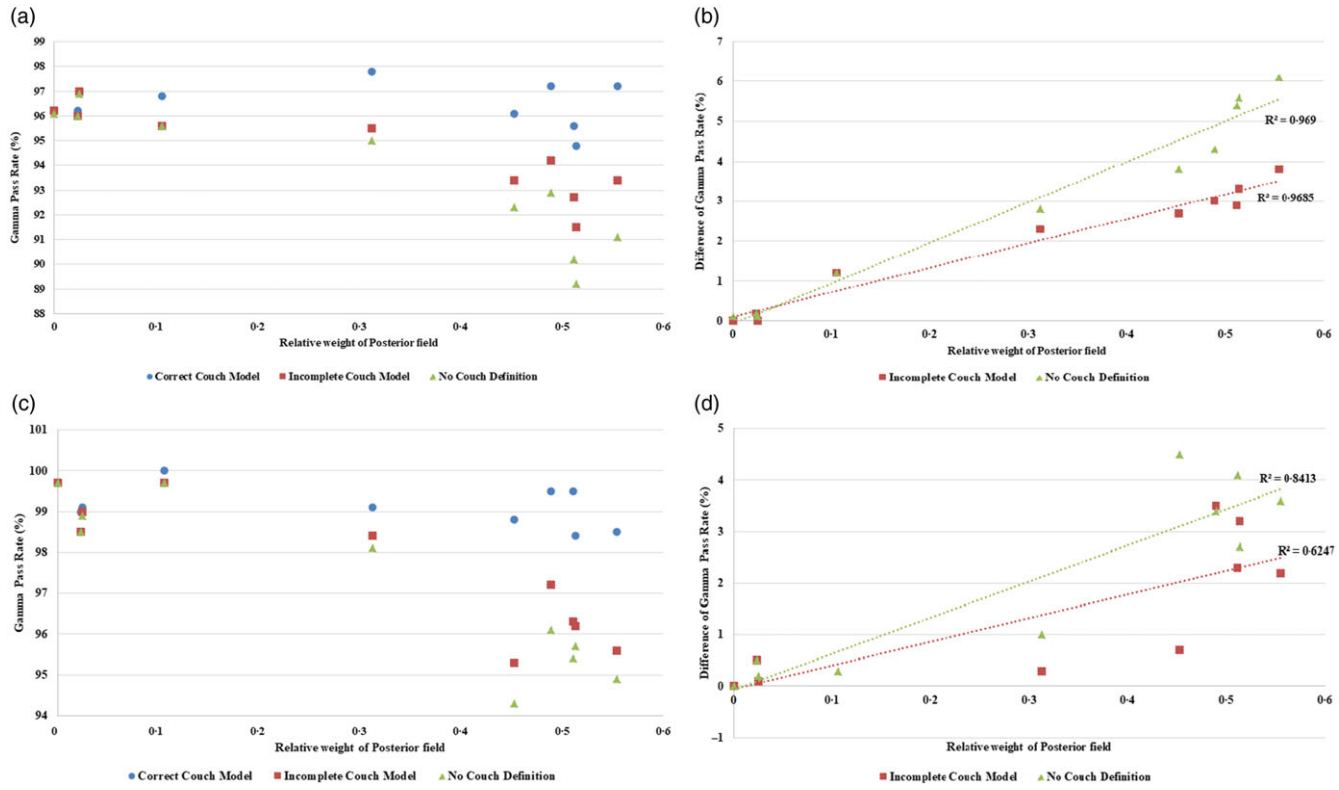

Figure 5. Differences of gamma pass rate values between the correct couch model with incomplete and no couch models versus these weight values of beams transmitting through the treatment couch. (a) Gamma pass rates of the QA plans with increasing the beam weights transmitting couch for all patients with 2%-2 mm gamma criteria. (b) Differences of gamma pass rate between the correct couch model with incomplete and not defined couch models in IMRT QA plans with 2%-2 mm gamma criteria. (c) Gamma pass rates of the QA plans with increasing the beam weights transmitting couch for all patients with 3%-3 mm gamma criteria. (d) Differences of gamma pass rates between the correct couch model with incomplete and not defined couch models in IMRT QA plans with 3%-3 mm gamma criteria.
R^2 values illustrate the linear trend lines fitted to the data of gamma pass rate differences.

of the couch by iPlan RT Dose TPS (3·4–9·5%) and Pinnacle TPS (2–6·6%) was within the same magnitude. Their modelled couch was relatively homogeneous, composed of carbon fibre outer shell filled with foam. However, the results of their study showed that posterior oblique fields have significantly higher attenuations compared to the posterior fields (9·5% versus 3·4% in iPlan RT Dose and 6·6% versus 2% in Pinnacle). In agreement with their study, we showed higher attenuation of posterior oblique fields compared to posterior fields (10–12% versus 2·1–3·4%).

In another study by Sedaghatian et al.,[9] the Siemens 550 TxT couch was evaluated to find its attenuation at different gantry angles. The model of this couch is different from our investigated couch and is relatively homogeneous, having an outer carbon fibre shell with hallow space. They reported maximum attenuation of 5·95% for 6 MV photon beam and field size of 5 × 5 cm^2 at 130° gantry angle (posterior oblique field). Our findings confirmed their results about higher attenuations of posterior oblique fields compared to the exact posterior field.

The effect of couch modelling on the gamma pass rate results depends on several factors, including the couch characteristics, gamma analysis criteria and weights of the fields transmitting through the couch. We compared the effect of two different gamma criteria (2%/2 mm versus 3%/3 mm) on the gamma pass rate results of comparing measured dose distribution with TPS calculations. In harder gamma analysis criteria (2%/2 mm), the effect of couch modelling was more prominent; therefore, correct couch modelling in the TPS is more important in plans with higher precisions. We obtained negative relationships between the weights of posterior beams and gamma pass rates of incomplete couch modelling for IMRT plans. However, no relation was observed if the couch was modelled correctly (inhomogeneous model) in the TPS. This means that correct modelling of treatment couch has a significantly higher effect in gamma pass rate results for plans having higher relative weights for posterior/posterior oblique fields. Assessing this relationship in VMAT plans is hard and time-consuming needs to evaluate the arclets irradiating in different gantry angles. However, in our opinion, similar relationships must have existed in the VMAT technique.

Conclusion

Inhomogeneous couches have different parts with different attenuations, which can be correctly defined using LINAC mounted CBCT. Modelling of treatment couch has a high effect on patient VMAT and IMRT delivery plans, especially in plans having radiation fields/subfield transmitting from the couch. Modelling the treatment couch using LINAC mounted CBCT, which is expressed in our study, is suggested for defining the geometry and materials of the treatment couch correctly in TPSs.

Acknowledgements. The authors wish to express their appreciation to the Negin Azadi oncology centre for their cooperation with providing the equipment used in this study.

https://doi.org/10.1017/S1460396921000716 Published online by Cambridge University Press

Funding. This research did not receive any specific grant from funding agencies in the public, commercial, or not-for-profit sectors.

Conflict of Interest. None.

References

1. Bortfeld T. IMRT: a review and preview. Phys Med Biol 2006; 51 (13): R363.
2. Goulet CC, Herman MG, Hillman DW, Davis BJ. Estimated limits of IMRT dose escalation using varied planning target volume margins. Phys Med Biol 2008; 53 (14): 3777.
3. Pollack A, Hanlon A, Horwitz EM, Feigenberg S, Uzzo RG, Price RA. Radiation therapy dose escalation for prostate cancer: a rationale for IMRT. World J Urol 2003;21 (4): 200–208.
4. De Mooy LG. The use of carbon fibres in radiotherapy. Radiother Oncol 1991; 22 (2): 140–142.
5. De Ost B, Vanregemorter J, Schaeken B, Van den Weyngaert D. The effect of carbon fibre inserts on the build-up and attenuation of high energy photon beams. Radiother Oncol 1997; 45 (3): 275–257.
6. Meara SJ, Langmack KA. An investigation into the use of carbon fibre for megavoltage radiotherapy applications. Phys Med Biol 1998; 43 (5): 1359.
7. Munjal RK, Negi PS, Babu AG, Sinha SN, Anand AK, Kataria T. Impact of 6MV photon beam attenuation by carbon fiber couch and immobilization devices in IMRT planning and dose delivery. J Med PhysicsAssociation Med Phys India 2006; 31 (2): 67.
8. Njeh CF, Parker J, Spurgin J, Rhoe E. A validation of carbon fiber imaging couch top modeling in two radiation therapy treatment planning systems: Philips Pinnacle 3 and BrainLAB iPlan RT Dose. Radiat Oncol 2012; 7 (1): 190.
9. Sedaghatian T, Momennezhad M, Rasta SH, Makhdoomi Y, Abdollahian S. An update of couch effect on the attenuation of megavoltage radiotherapy beam and the variation of absorbed dose in the build-up region. J Biomed Phys Eng 2017; 7 (3): 279.
10. Klein EE, Hanley J, Bayouth J et al. Task group 142 report: quality assurance of medical acceleratorsa. Med Phys 2009; 36 (9Part1): 4197–4212.
11. Chen J, Morin O, Aubin M, Bucci MK, Chuang CF, Pouliot J. Dose-guided radiation therapy with megavoltage cone-beam CT. Br J Radiol 2006; 79 (special_issue_1): S87–S98.
12. Li Y, Netherton T, Nitsch PL et al. Normal tissue doses from MV image-guided radiation therapy (IGRT) using orthogonal MV and MV-CBCT. J Appl Clin Med Phys 2018; 19 (3): 52–57.
13. Held M, Cremers F, Sneed PK et al. Assessment of image quality and dose calculation accuracy on kV CBCT, MV CBCT, and MV CT images for urgent palliative radiotherapy treatments. J Appl Clin Med Phys 2016; 17 (2): 279–290.
14. Ezzell GA, Burmeister JW, Dogan N, et al. IMRT commissioning: multiple institution planning and dosimetry comparisons, a report from AAPM Task Group 119. Med Phys 2009; 36 (11): 5359–5373.
15. Mans A, Schuring D, Arends MP et al. The NCS code of practice for the quality assurance and control for volumetric modulated arc therapy. Phys Med Biol 2016; 61 (19): 7221.
16. Allgaier B, Schüle E, Würfel J. Dose reconstruction in the OCTAVIUS 4D phantom and in the patient without using dose information from the TPS. White Pap 2013. https://www.ptw.de/fileadmin/data/download/publications/OCTAVIUS_4D_White_Paper_Note_en_91320006_00.pdf.
17. Kunz G, Hasenbalg F, Pemler P. Absorption measurements for a carbon fiber couch top and its modelling in a treatment planning system. SSRMP Annu Scan Line Mm 0 2010; 20: 40–60.
18. Sheykhoo A, Abdollahi S, Yazdi MHH, Ghorbani M, Mohammadi M. Effects of Siemens TT-D carbon fiber table top on beam attenuation, and build up region of 6 MV photon beam. Rep Pract Oncol Radiother 2017; 22 (1): 19–28.
19. Schmidhalter D, Fix MK, Wyss M et al. Evaluation of a new six degrees of freedom couch for radiation therapy. Med Phys 2013; 40 (11): 111710.

https://doi.org/10.1017/S1460396921000716 Published online by Cambridge University Press

Appendix A:

Field by field (arc by arc) gamma analysis results for each patient are shown in Tables A1 and A2 for two assessed gamma analysis limitations and both of the IMRT (Table A2) and VMAT (Table A2) techniques.

Table A1. Gamma pass rates for each field at two assessed gamma analysis limitations in IMRT QA plans for correct, incomplete and no-defined couch models for all patients

Cancer site irradiation energy, and prescription	Fields	Gantry angle	Delivered dose to isocentre (Gy)	Gamma pass rate (%) Condition: 2% & 2 mm			Gamma pass rate (%) Condition: 3% & 3 mm		
				Correct couch definition	Incomplete couch definition	No couch definition	Correct couch definition	Incomplete couch definition	No couch definition
Neck 6 MV 2 Gy × 25 fr	1	0	0·303	96·4	96·5	96·4	99·6	99·5	99·6
	2	35	0·414	96·3	96·3	96·2	99·5	99·5	99·5
	3	70	0·505	96·5	96·5	96·5	99·7	99·7	99·7
	4	325	0·401	96·2	96·3	96·2	99·8	99·8	99·8
	5	290	0·471	96·2	96·2	96·1	99·6	99·6	99·6
	All	–	2	96·2	96·2	96·1	99·7	99·7	99·7
Larynx 6 MV 1·8 Gy × 25 fr	1	180	0·045	95·5	93·8	93·8	98·7	97·9	97·8
	2	30	0·298	96·1	96·1	96·1	99	99	99
	3	60	0·324	96·4	96·4	96·4	99·4	99·4	99·4
	4	90	0·329	96·3	96·3	96·3	99·8	99·8	99·8
	5	270	0·332	95·9	95·9	95·9	99·7	99·7	99·7
	6	300	0·348	95·3	95·3	95·3	98·9	98·9	98·9
	7	330	0·25	96·8	96·8	96·8	99·3	99·3	99·3
	All	–	1·8	96·2	96	96	99	98·5	98·5
Larynx 6 MV 1·8 Gy × 25 fr	1	180	0·046	97	96·8	95·9	99·8	99·4	99
	2	30	0·135	97·4	97·4	97·4	100	100	100
	3	60	0·286	97·5	97·5	97·5	99·7	99·7	99·7
	4	90	0·425	97·5	97·5	97·5	100	100	100
	5	270	0·502	97·5	97·5	97·5	99·8	99·8	99·8
	6	300	0·32	97·2	97·2	97·2	99·6	99·6	99·6
	7	330	0·136	97	97	97	99·7	99·7	99·7
	All	–	1·8	97	97	96·9	99·1	99	98·9
Brain Met 6 MV 2·67 Gy × 15 fr	1	0	0·487	97·3	97·3	97·2	99·7	99·7	99·7
	2	41	0·267	96·8	96·8	96·8	99·9	99·9	99·9
	3	81	0·267	94·3	94·3	94·3	99·6	99·6	99·6
	4	121	0·042	95	83	82·4	99·5	94·1	93·6
	5	161	0·112	94·1	92·1	92·1	99·6	98·9	98·9
	6	201	0·017	96·1	85·9	86	99·7	98·3	98·3
	7	241	0·059	86·5	83·1	81·2	97·6	95·1	92·3
	8	281	0·508	96·3	96·3	96·2	99·3	99·3	99·3
	9	321	0·412	93·2	93·2	98·2	99·2	99·2	99·2
	All	–	2·67	96·8	95·6	95·6	100	99·7	99·7

(*Continued*)

https://doi.org/10.1017/S1460396921000716 Published online by Cambridge University Press

Table A1. (*Continued*)

Cancer site irradiation energy, and prescription	Fields	Gantry angle	Delivered dose to isocentre (Gy)	Gamma pass rate (%) Condition: 2% & 2 mm			Gamma pass rate (%) Condition: 3% & 3 mm		
				Correct couch definition	Incomplete couch definition	No couch definition	Correct couch definition	Incomplete couch definition	No couch definition
Prostate, pelvic 6 MV 2 Gy × 23 fr	1	0	0·087	98·1	98·1	98·1	99·7	99·7	99·7
	2	50	0·289	98·5	98·5	98·5	99·4	99·4	99·4
	3	100	0·365	97·9	97·4	97·1	98·9	98·6	98·5
	4	130	0·282	96·5	92·3	91·5	98·8	94·3	92·2
	5	230	0·287	96·4	91·8	91·1	98·5	93·8	92
	6	260	0·366	97·7	97·3	97·3	99·1	98·8	98·5
	7	300	0·143	97·8	97·8	97·8	99·5	99·5	99·5
	All	–	2	97·8	95·5	95	99·1	98·4	98·1
Parotid 6 MV 1·82 Gy × 33 fr	1	0	0·273	97·2	97·2	97·2	99·3	99·3	99·3
	2	321	0·305	96·4	96·4	96·4	98·6	98·6	98·6
	3	281	0·428	96·7	96·7	96·7	99·1	99·1	99·1
	4	241	0·419	97·2	93·4	91·2	99·5	95·5	93·8
	5	171	0·251	96	94·6	94·9	98·3	96·7	96·4
	6	141	0·163	93·6	89·3	87·2	97·9	92·5	91·1
	All	–	1·82	96·1	93·4	92·3	98·8	95·3	94·3
Tongue 6 MV 2 Gy × 30 fr	1	180	0·155	97·3	94·8	94	99·8	97·7	96·6
	2	221	0·273	96·1	92·2	90·1	98·5	96·1	95·7
	3	261	0·183	97·3	95·1	94·9	99·5	98·2	98·2
	4	301	0·042	96·5	96·5	96·5	99·3	99·3	99·3
	5	341	0·57	96·3	96·3	96·3	99·3	99·3	99·3
	6	21	0·354	97·4	97·4	97·4	100	100	100
	7	61	0·119	96·5	96·5	96·5	99	99	99
	8	101	0·128	96·9	94·7	93·9	99·6	97·6	97·3
	9	141	0·301	96·6	91·4	90·3	99·2	96·3	95·2
	All	–	2	97·2	94·2	92·9	99·5	97·2	96·1
GBM, brain 6 MV 2 Gy × 27 fr	1	180	0·102	95·8	93·8	93·8	98·6	97·5	97·5
	2	210	0·263	95·4	89·1	85·2	99·7	95·4	94·6
	3	240	0·174	94·4	87·4	82·7	98·5	94·6	92·7
	4	270	0·253	95·5	95·4	95·5	98·8	98·8	98·8
	5	300	0·337	95	95	95·1	99·3	99·3	99·3
	6	150	0·229	94·7	86·5	82·1	99·8	96·3	95·5
	7	85	0·153	96·1	96·1	96·1	99·9	99·9	99·9
	8	280	0·485	95·3	95·3	95·3	99·3	99·3	99·3
	All	–	2	95·6	92·7	90·2	99·5	96·3	95·4
Bladder, 6 MV 1·8 Gy × 28 fr	1	0	0·185	95·1	95·1	95·1	98·6	98·6	98·6
	2	60	0·402	96·3	96·3	96·3	100	100	100
	3	100	0·226	94·2	93·5	93	98·4	98·1	98·1
	4	140	0·269	94·1	88·6	85·4	98·7	93·3	92·9
	5	220	0·274	92·8	85·3	83·1	99·5	94·5	94·2
	6	260	0·238	96·6	94·8	94·2	98·9	97·7	97·4
	7	300	0·365	96·5	96·5	96·5	99·2	99·2	99·2
	All	–	1·8	94·8	91·5	89·2	98·4	96·2	95·7

(*Continued*)

https://doi.org/10.1017/S1460396921000716 Published online by Cambridge University Press

Table A1. (*Continued*)

Cancer site irradiation energy, and prescription	Fields	Gantry angle	Delivered dose to isocentre (Gy)	Gamma pass rate (%) Condition: 2% & 2 mm			Gamma pass rate (%) Condition: 3% & 3 mm		
				Correct couch definition	Incomplete couch definition	No couch definition	Correct couch definition	Incomplete couch definition	No couch definition
Larynx 6 MV 1·8 Gy × 25 fr	1	180	0·054	96·7	93·2	93·1	99·5	95·5	93·5
	2	221	0·208	93·2	87·5	84·4	97·6	93·8	90·5
	3	261	0·245	94·3	91·5	90·8	98·8	95·4	94·9
	4	301	0·238	95·5	95·5	95·5	98·8	98·8	98·8
	5	341	0·143	95·8	95·8	95·8	99	99	99
	6	21	0·193	95·1	95·1	95·1	98·7	98·7	98·7
	7	61	0·229	96·3	96·3	96·3	99·5	99·5	99·5
	8	101	0·274	97·2	94·9	94·3	99·4	95·8	94·6
	9	141	0·22	97·1	87·1	81·6	96·1	91·3	89·8
	All	–	1·8	97·2	93·4	91·1	98·5	95·6	94·9

Table A2. Gamma pass rates for each arc at two assessed gamma analysis limitations in VMAT QA plans for correct, incomplete and no-defined couch models for all patients

Cancer site, irradiation energy, and prescription	Arcs	Arc angle range	Delivered dose	Gamma pass rate (%) Condition: 2% & 2 mm)			Gamma pass rate (%) Condition: 2% & 2 mm		
				Correct couch definition	Incomplete couch definition	No couch definition	Correct couch definition	Incomplete couch definition	No couch definition
Sacrum, 6 MV, 1.8 Gy × 25 fr	1	250 to 110 CW	0·948	97·8	95·8	94·6	99·6	97·1	96·3
	2	110 to 250 CCW	0·902	97·3	95·5	94·8	99·3	97·4	96·5
	All	–	1·8	97·5	95·6	94·7	99·4	97·2	96·3
Brain, SRS,7 MV, 8 Gy × 4 fr	1	181 to 340 CW	3·108	97·0	91·6	88·1	100	94·5	92·2
	2	181 to 60 CCW	1·848	96·8	92·7	90·0	99·9	95·4	93·8
	3	330 to 181 CCW	0·973	96·8	92·3	90·4	100	94·7	91·7
	4	179 to 30 CCW	1·221	97·1	94·8	92·6	100	96·4	95·7
	5	181 to 330 CW	2·310	96·7	91·8	90·14	99·4	95·8	95·1
	All	–	8	97·1	92·6	90·2	99·8	95·4	93·8
Brain, SRS, 7 MV, 5 Gy × 5 fr	1	181 to 179 CW	1·694	96·2	95·9	94·9	99·5	96·8	96·0
	2	179 to 181 CCW	1·966	96·3	95·7	95·1	99·8	96·5	95·5
	3	179 to 0 CCW	1·146	95·4	93·5	92·2	98·7	95·2	93·1
	4	0 to 181 CCW	0·807	96·5	95·4	92·5	99·6	95·7	93·4
	5	181 to 0 CW	0·855	96·3	94·8	92·0	99·8	95·1	94·5
	All	–	5	96·1	95·3	92·3	99·7	95·4	94·5
Pelvic,7MV, 2 Gy × 25 fr	1	182 to 178 CW	0·969	97·7	96·2	95·8	99·7	98·2	98·0
	2	178 to 182 CCW	1·244	96·1	94·0	93·2	99·1	97·8	97·5
	All	–	2	97·2	94·5	93·8	99·0	97·3	97·2
Brain, 7MV, 2 Gy × 27 fr	1	181 to 179 CW	0·930	97·7	95·6	94·5	98·9	96·1	93·8
	2	179 to 0 CCW	0·271	98·4	94·1	93·1	99·2	96·4	94·3
	3	0 to 181 CCW	0·179	98·8	95·7	94·4	100	96·4	94·3
	4	181 to 0 CW	0·633	99·2	95·9	94·1	100	96·5	94·2
	All	–	2	97·3	95·5	93·7	100	96·4	94·2

(*Continued*)

https://doi.org/10.1017/S1460396921000716 Published online by Cambridge University Press

Table A2. (*Continued*)

Cancer site, irradiation energy, and prescription	Arcs	Arc angle range	Delivered dose	Gamma pass rate (%) Condition: 2% & 2 mm)			Gamma pass rate (%) Condition: 2% & 2 mm		
				Correct couch definition	Incomplete couch definition	No couch definition	Correct couch definition	Incomplete couch definition	No couch definition
Brain SRS 4·2 Gy × 4 fr	1	181 to 179 CW		98·0	95·1	94·2	99·5	97·2	95·4
	2	179 to 0 CCW		98·3	96·0	94·8	99·7	97·6	95·9
	3	0 to 181 CCW		97·2	94·7	92·6	98·6	96·3	95·3
	4	181 to 0 CW		98·4	95·5	93·7	100	97·4	96·0
	All	–		98·1	95·6	93·2	99·3	96·8	95·6
Thoracic spine paraspine, 7 MV, 2 Gy × 33 fr	1	182 to 178 CW	0·987	98·6	96·4	95·2	100	97·8	95·2
	2	178 to 182 CCW	1·103	99·2	96·0	94·1	100	96·9	94·9
	All	–	2	99·4	96·0	94·4	100	97·4	95·0
Brain, SRS, 7 MV, 4·2 Gy × 5 fr	1	181 to 179 CW	0·185	95·7	92·2	91·0	97·6	94·8	93·2
	2	179 to 181 CCW	0·236	96·4	93·1	91·4	98·8	95·3	93·6
	3	179 to 0 CCW	0·430	96·6	92·3	90·8	98·6	95·6	92·7
	4	0 to181 cCW	0·037	96·0	91·4	88·6	99·1	97·5	89·9
	5	181 to 0 CW	0·967	96·5	92·3	89·7	98·3	95·2	91·0
	All		4·2	96·7	92·8	90·2	98·4	95·5	91·4
GBM, brain, 6 MV, 2 Gy × 30 fr	1	181 to 179 CW	0·609	97·6	95·8	93·9	98·9	97·2	95·8
	2	179 to 0 CCW	0·757	98·7	96·2	93·5	99·6	97·8	96·7
	3	0 to 181 CCW	0·597	98·3	96·2	94·6	99·3	97·5	95·5
	4	181 to 0 CW	0·215	97·6	95·1	92·8	98·5	96·6	94·3
	All		2	98·3	95·6	93·8	99·2	97·1	95·6
Brain, optic nerve meningioma, 7 MV, 5 Gy × 5 fr	1	5 to 188 CW	1·875	97·6	95·8	94·3	99·5	96·9	95·0
	2	173 to 10 CCW	1·354	97·8	95·8	94·1	99·5	96·8	95·2
	3	175 to 10 CCW	1·924	98·2	96·7	94·7	100	97·2	95·6
	4	10 to 175 CW	0·946	97·2	94·9	93·3	99·4	96·3	94·8
	All		5	97·9	95·4	94·0	99·7	96·7	95·2
Brain, GBM, 7 MV, 3·4 Gy × 10 fr	1	181 to 179 CW	1·708	97·4	93·2	91·6	100	96·6	94·8
	2	179 to 0 CCW	0·998	97·3	93·4	91·6	99·6	96·4	94·5
	3	181 to 0 CW	0·919	97·7	95·2	92·6	100	97·1	94·9
	All		3·4	97·5	94·3	91·8	99·7	96·8	94·5
Prostate, pelvic, 6 MV, 2 Gy × 25 fr	1	181 to 179 CW	0·466	96·8	94·2	93·0	98·9	96·1	94·1
	2	179 to 181 CCW	0·699	97·5	95·8	94·2	99·5	96·8	95·3
	3	181 to 179 CW	0·466	96·9	95·0	93·8	99·4	96·2	94·9
	All		2	97·4	95·0	93·7	99·2	96·5	94·9

https://doi.org/10.1017/S1460396921000716 Published online by Cambridge University Press